

# Dendronized Polymers: Molecular Objects between Conventional Linear Polymers and Colloidal Particles

A. Dieter Schlüter,<sup>\*,†</sup> Avraham Halperin,<sup>\*,‡</sup> Martin Kröger,<sup>§</sup> Dimitris Vlassopoulos,<sup>||,⊗</sup> Gerhard Wegner,<sup>⊥</sup> and Baozhong Zhang<sup>†,‡,‡</sup>

<sup>†</sup>Laboratory of Polymer Chemistry, Department of Materials, ETH Zurich, 8093 Zurich, Switzerland

<sup>‡</sup>Laboratoire de Spectrométrie Physique (LSP), CNRS Université Joseph Fourier, BP 87, 38402 Saint Martin d'Hères cedex, France

<sup>§</sup>Polymer Physics, Department of Materials, ETH Zurich, 8093 Zurich, Switzerland

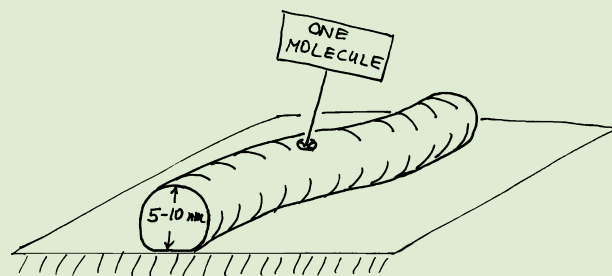
<sup>||</sup>Institute of Electronic Structure and Laser, Foundation for Research and Technology (FORTH), 71110 Heraklion, Crete, Greece

<sup>⊗</sup>Department of Materials Science & Technology, University of Crete, 71003 Heraklion, Crete, Greece

<sup>⊥</sup>Max-Planck-Institute for Polymer Research, Ackermannweg 10, 55128 Mainz, Germany

<sup>#</sup>Lund University, Centre of Analysis and Synthesis, P.O. Box 124, SE-22100 Lund, Sweden

**ABSTRACT:** The term molecular object (MO) is introduced to describe single, shape persistent macromolecules that retain their form and mesoscopic dimensions irrespective of solvent quality and adsorption onto a surface. The concept is illustrated with results concerning homologous series of dendronized polymers (DP). In particular, we discuss imaging experiments quantifying deformation upon adsorption, defect characterization, and atomistic molecular dynamics simulations of DP structure. We argue that MOs such as high generation DP, with their large dimensions and high internal density, provide an opportunity to address fundamental questions regarding the onset of bulk-like behavior in single molecules. Illustrative examples of such questions concern the smallest MO exhibiting a glass transition, glassy behavior or a constant bulk density. The characteristics of DP MO are highlighted by comparison to polymer beads, polymeric micelles, globular proteins, and carbon nanotubes. We discuss future research directions and speculate on possibilities involving multiarmed and toroid DP and the effect of DP on friction and rheology, as well as their utilization for nanoconstruction.



Let us start with a Gedankenexperiment before going into what dendronized polymers (DP) are and why we propose to describe some of them as molecular objects (MO). Imagine that a heavily cross-linked plastic rod is machined down into a cylinder with mesoscopic dimensions; say a diameter of 10 nm and a length of 1  $\mu\text{m}$ . If the cross-link density is high, one can assign a volume and a surface to this imaginary cylinder. Furthermore, the cylinder has a shape, a particular mass density, certain deformability, and capacity to swell. In solution two such cylinders interact as rigid rods, resembling hard-core colloidal particles. Is this tiny plastic cylinder an object? Familiar day-to-day objects such as a pen, rubber band, or cup have a defined volume and shape as well as a function. The surface of an object, for example, the glaze on a porcelain cup, separates the interior (ceramics) from the exterior (air and coffee) very much, as is the case for our cylinder. Obviously the porcelain cup has negligible deformability and does not swell, being a hard matter object. In contrast, soft matter objects such as rubber bands can deform and swell. Our imaginary cylinder thus exemplifies a soft matter nano-object irrespective of its utility, an issue we will revisit later. It serves to motivate our quest to down-size multimolecular macroscopic objects and to create monomolecular nano-objects which can be visualized

and manipulated by AFM. This brings us to the definition of a MO we will use in the following. MO is a nanoscale or mesoscopic scale particle having the following properties: it (1) consists of a single molecule, (2) has an intrinsic shape defined by a sharp interface, and (3) is shape-persistent in the sense that it retains its shape irrespective of solvent quality for example upon adsorption to a solid substrate. We use the term intrinsic shape to denote shape due to molecular structure as obtained without recourse to extrinsic factors such as molds or templates. This requirement excludes rubber tires and similarly cross-linked network objects that have no intrinsic shape, such as single chain nanoparticles (SCNP).<sup>1,2</sup> The currently reported SCNPs have no intrinsic shape nor are there yet examples of SCNPs having a persistent shape. For the purpose of our discussion, the requirement for shape persistency is not limited to the trajectory of the polymer, as described by persistence length, but also concerns the molecular cross-section. In this article we focus on MOs of mesoscopic size<sup>3</sup> as encountered in colloid science and biology.<sup>4,5</sup> With this definition in mind, our

**Received:** June 23, 2014

**Accepted:** September 5, 2014

**Published:** September 15, 2014

imaginary cylinder is not an MO, being multimolecular. We should add that a number of chemical structures such as fullerenes and carbon nanotubes (CNT) incorporate surface-delimited pores of well-defined shape, and such pores can also be considered as a structural feature of MOs.

Along this line of thought, one of us (ADS) initiated in 1993 a program to develop synthetic chemistry to create mesoscopic MOs.<sup>6</sup> The idea was to avoid self-assembly and random cross-linking and to create both size and shape solely via carefully placed covalent bonds. The realization of this program imposed two requirements: The first is an element of shape creation built into the chemical structures generated by the synthesis. The second is a choice of chemistry ensuring the highest structural perfection even when executed hundreds of thousand times for one and the same molecule. This is the point where DPs enter the discussion.<sup>7–9</sup> These macromolecules are comb-like polymers in which the teeth of the comb are not linear, as in conventional bottlebrush polymers,<sup>10–13</sup> but rather regularly branched, tree-like units, referred to as dendrons.<sup>14</sup> Figure 1a

depicts the molecular structure of a representative **PG5**, which is a DP of generation  $g = 5$  having a backbone comprising  $n$  repeat units. This macromolecule, with its huge substituents on every backbone repeat unit of length 2.5 Å, immediately brings out the concept behind the molecular design: shape creation by steric repulsion. Let us now have a closer look at this structure.<sup>15</sup> **PG5** is a  $g = 5$  DP because it consists of dendrons with five consecutive branching points. The backbone chain contour length can be tuned from a few tens of nm to a few  $\mu\text{m}$ . The particular, **PG5**, reported in ref 15, has an average backbone polymerization degree of  $n = 10600$ , with an average contour length  $L = 2.6 \mu\text{m}$ . Its cross-sectional diameter  $D$  in the dry state is  $D \approx 7.5 \text{ nm}$ , demonstrating a large “thickness” (see below), unheard of among common polymers.<sup>15</sup>

Figure 1b also displays the key chemical equation describing the synthesis of DPs by a step-by-step,  $g$ -by- $g$  procedure. It is founded on a divergent growth strategy, first described by Vögtle<sup>16</sup> and later applied to dendrimers by Tomalia,<sup>17</sup> using a robust amidation chemistry based upon the active ester dendronization reagent **DG1**. Such chemistry dates back to Merrifield’s famous peptide syntheses.<sup>18</sup> The particular reaction sequence shown describes the conversion **PG1** to **PG2**, but it can be repeated over and over again. It thus provides access to a homologous series of DPs whose members all have the same backbone chain length and length distribution but differ in  $g$ , in shape-persistence and cross-sectional diameter. **PG5** was obtained in exactly this way.

Each DP is a linear array of laterally crowded dendrons whose strands are flexible enough to backfold toward the backbone. In other words, it is a bottlebrush polymer with repeatedly branched dendron side chains. A more detailed description of the configurations and interactions of DPs depends on the actual molecular structure,  $g$ , and solvent quality. In any case, the diameter of DPs increases with  $g$ : the larger the  $g$ , the more spatially demanding are the dendrons and the thicker is the polymer. The creation of persistent shape is due to the combination of placing an enormous mass into the small volume available to densely branched dendrons and the dendrons’ narrow spacing along the backbone. It is this very combination of factors which sets high- $g$  DPs apart from common linear polymers with regard to their ability to form molecular objects of mesoscopic dimensions.

In discussing the shape of DPs we consider two aspects, namely, the backbone trajectory and the cross-section of the DP. Locally, the unperturbed DP is cylindrical with a circular cross-section of diameter  $D$ . The chain is essentially rod like on length scales below the persistence length  $\lambda \sim D^2$ .<sup>19,20</sup> DPs of length  $L \gg \lambda$  ultimately behave as flexible chains. Since our primary interest is in MO we often focus on the  $L \leq \lambda$  range where DPs behave as bendable rods. It is now necessary to consider  $D$  at greater detail because for low  $g$  it does not depend only on  $g$  but also on the physical state of the DP. It matters whether this macromolecule is in melt or in solution, if it is adsorbed on a solid substrate, or if it is freely moving in outer space. When adsorbed on a substrate, the DP cross-section is deformed by substrate induced flattening and its diameter is no longer defined. The intrinsic  $D$  is only observed under high vacuum condition, the ultimate poor solvent, when all branches are collapsed into a dense configuration. Figure 1c depicts the results of molecular dynamics (MD) simulations for **PG1–PG6** in vacuum. One can immediately perceive the effect of increasing  $g$  on the densely packed structures and the associated increase of the shape-persistence and  $D$ .<sup>21–23</sup> As we

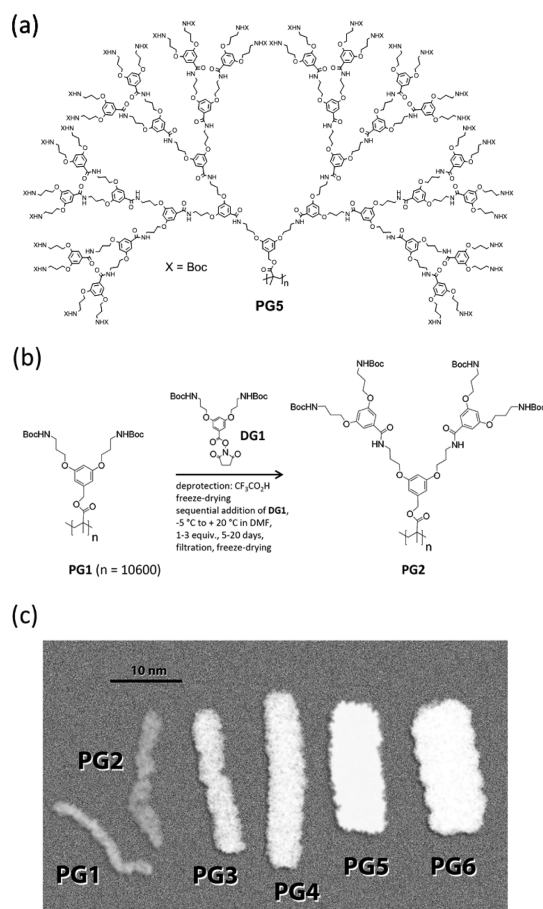


**Figure 1.** Structures and synthesis route of dendronized polymers (DPs). (a) Chemical structure of the fifth generation ( $g = 5$ ) DP **PG5**. This macromolecule has on average  $n = 10600$  repeat units. (b) A typical divergent growth step to create the  $(g + 1)$  DP from  $g$  DP. It is based on active ester chemistry through which the  $g = 1$  dendronization agent **DG1** is hooked on to each of the terminal amine groups of the starting DP. These free amines are first generated from the neutral *tert*-butoxycarbonyl (Boc) protected starting DP. The specific sequence shown is for the conversion **PG1** to **PG2**. (c) Snapshots of structures of **PG1–PG6** with different numbers of repeat units as obtained from MD simulations in vacuum (adapted from ref 22) for  $n$  in the range of 100–150, indicating locally cylindrical shape.

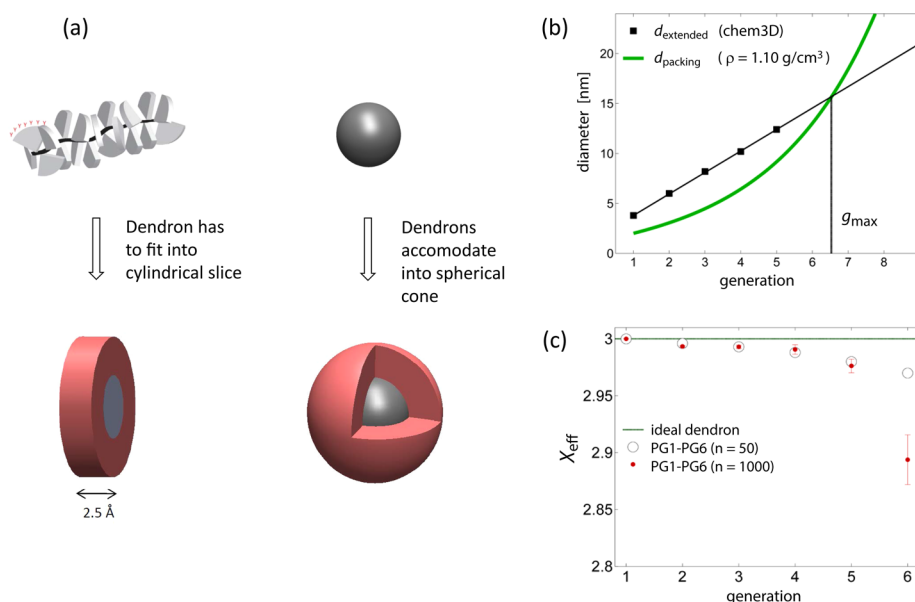


**Figure 2.** Available space and defects in DPs. (a) For DPs the dendron has to fit into cylindrical slices of width determined by the length of a backbone repeat unit (2.5 Å). On the other hand, for dendrimers, the dendrons are accommodated into a spherical cone, thus, causing less steric congestion. Accordingly,  $g_{\text{max}}$  of DP is reached at much lower  $g$  than for dendrimers. (b) The  $g_{\text{max}}$  is identified as the intersect between the straight line of the  $g$ -dependent maximal possible cross-sectional diameter and the exponential curve of the  $g$ -dependent diameter of the collapsed DP. (c) The effective number of junction-junction bonds per inner junction,  $X_{\text{eff}}$ , as calculated from the experimental labeling data.<sup>35</sup> Depicted are the curves obtained for  $n \approx 50$  and  $n \approx 1000$  as well as the prediction for the ideal dendron characterized by  $X_{\text{eff}} \lesssim 3$ . For  $g < 5$  the two data sets are basically indistinguishable and well described by a constant reaction efficiency  $P = 0.995$ .<sup>27</sup> The onset of SIS is evident from the difference between  $n \approx 50$  and  $n \approx 1000$  at  $g = 6$ ; the effective number of bonds is reduced from 3 to 2.89, thus supporting onset of steric crowding.

have discussed, the shape of low- $g$  DPs is sensitive to the environment. This is manifested by their response to solvent quality and adsorption to a surface. In particular, low  $g$  DP swell in solvents and their  $D$  varies with solvent quality.

In view of our definition of MO why do we even consider DPs as candidates? One requires a MO to retain its shape when adsorbed onto an attractive surface and not to swell when dissolved in a good solvent. Can DPs exhibit such lack of response to environmental conditions? To address this question we need to discuss what happens to DPs when  $g$  increases until  $g_{\text{max}}$  and the maximal attainable density is reached. The concept of  $g_{\text{max}}$  was introduced by de Gennes and Hervet in their seminal 1983 article on dendrimers.<sup>24</sup> In its original form it specifies the maximal generation up to which structurally *perfect* dendrons can still be accommodated around the core (for dendrimers) or the backbone (for DPs). Beyond  $g_{\text{max}}$ , defect-free structures are impossible because of steric packing constraints. These arise because of the interplay of two factors. First, the maximal attainable dendron span, as determined by the length of a fully extended strand, increases linearly with  $g$ . Second the diameter of a collapsed, defect-free DP increases exponentially reflecting the mass growth (Figure 2). The two curves intersect at  $g_{\text{max}}$ . Although for  $g < g_{\text{max}}$  there is still space available for growth and solvent uptake within the branches, at  $g = g_{\text{max}}$ , the point is reached where the branches for the first time fill up the entire available volume, given the limitations imposed by the molecular structure. DPs and dendrimers with  $g > g_{\text{max}}$  can in principle be synthesized but only at the price of branching defects.<sup>25–27</sup> The discussion of  $g_{\text{max}}$  for structurally perfect dendritic molecules assumes complete conversion of the add-on reaction in the absence of steric congestion. The argument can be generalized to allow for incomplete but constant reaction efficiency. With such pictures

$g_{\text{max}}$  emerges as a sharp boundary between two synthetic regimes such that at low  $g$  the add-on reaction is chemistry controlled while for high  $g$  it is controlled by steric packing effects. For  $g \leq g_{\text{max}}$ , the synthesis proceeds with the coupling efficiency of model add-on reactions free of steric hindrance. In contrast, for  $g > g_{\text{max}}$  the coupling efficiency is reduced by steric constraints imposing branching defects. As a result the effective functionality of the inner junctions is reduced for  $g > g_{\text{max}}$ , approaching 2 in the limit of very high  $g$ . This global form of steric hindrance associated with  $g \geq g_{\text{max}}$ ,<sup>27</sup> referred to by Tomalia as sterically induced stoichiometry (SIS),<sup>25,26</sup> corresponds to a situation where chemical reactions within a dense, highly branched structure cannot proceed because of lack of available space. Beyond  $g_{\text{max}}$ ,<sup>27</sup> DPs are expected to be as tightly packed as their molecular structure allows and their ability to accommodate solvent molecules is reduced. This is also the range where the molecular structure of a DP is anticipated to exert its largest impact in terms of shape creation.<sup>28</sup> Below  $g_{\text{max}}$ , shape reflects the interplay between configurational entropy and excluded volume interactions and it thus varies with solvent quality and adsorption.<sup>29,30</sup> At  $g \geq g_{\text{max}}$  we expect DPs to retain their locally cylindrical shape but with a diameter that does not vary with solvent quality or adsorption. This is in contrast to macromolecules that assume a cylindrical form only under certain conditions as exemplified by bottlebrush polymers, with linear side chains, that are locally cylindrical when free in solution but flatten out when adsorbed onto a solid surface. Another such example are low  $g$  DPs carrying mesogenic side chains that assemble into cylindrical phases in the solid state, structures that disappear upon melting, as was shown by Percec.<sup>31</sup>

Is the experimental exploration of the  $g \geq g_{\text{max}}$  range feasible? There are two issues involved. One concerns the observable

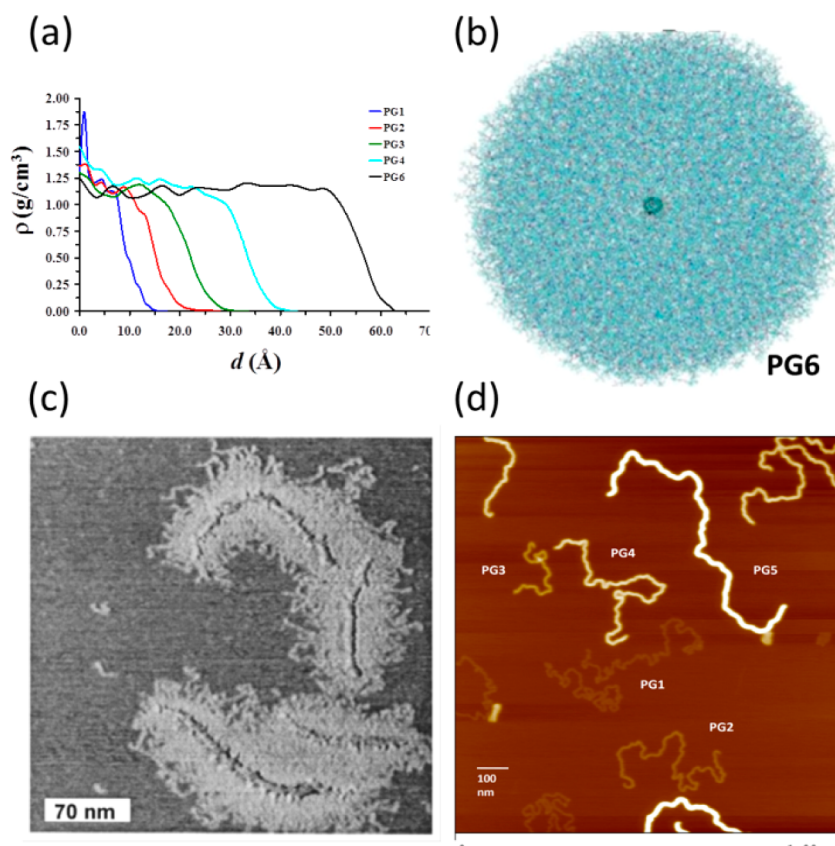


**Figure 3.** On the shape of DPs and bottlebrush polymers. (a) Simulated radial density profile of PG1–PG4 and PG6 in vacuum and (b) cross-section image of PG6. (c) AFM images of bottlebrush polymers on mica and (d) coprepared PG1–PG5 DPs on mica.

signatures of SIS in this range. Within the simple picture described above,<sup>24,27</sup>  $g_{\max}$  identifies a sharp threshold for the onset of SIS, that is, the efficiency of the add-on reaction changes abruptly at  $g_{\max}$ . In this approach, one sees that packing constraints impose SIS above  $g_{\max}$  and assumes no steric hindrance below  $g_{\max}$ . However, the steric environment encountered at different reaction sites is not identical thus suggesting that the transition between the two synthetic regimes occurs gradually over a  $g$  interval,  $\Delta g$ , bracketing  $g_{\max}$ . Such behavior was indeed observed in Monte Carlo (MC) simulation using a kinetic growth model.<sup>27</sup> The experimental exploration of the  $g \geq g_{\max}$  range depends on the width of  $\Delta g$  and the corresponding variation in the add-on reaction efficiency. Evidently, an efficient add-on reaction at low  $g$  with a narrow  $\Delta g$  is most favorable in order to obtain clear results. We will return to this point shortly. The second issue relates to the practical synthetic accessibility of the  $g \geq g_{\max}$  range. To identify  $g_{\max}$  as well as quantify SIS effects at  $g > g_{\max}$  and the corresponding effects on shape, it is necessary to produce a homologous series extending to beyond the crossover range, that is, up to  $g > g_{\max} + \Delta g$ . The associated synthetic difficulties grow with  $g$ , thus, favoring the exploration of systems with lower  $g_{\max}$ . This last point is advantageous for cylindrical DPs where  $g_{\max}$  is lower than  $g_{\max}$  of the corresponding dendrimers whose spherical shape weakens steric congestion (Figure 2).<sup>28,32–34</sup> As we shall discuss below, the emerging experimental evidence suggests that the  $g \geq g_{\max}$  range is within reach. In particular, the estimated  $g_{\max}$  of the above DPs is between  $g = 6–7$ , while for similar dendrimers,  $g_{\max}$  occurs at  $g > 10$ . PG6 is thus close to the predicted  $g_{\max}$ .

Having argued that MOs are attained at the vicinity of  $g_{\max}$  as signaled by the onset of SIS it is important to have a method to quantify branching defects. For our chemistry nonreacted primary amines are associated with the single possible type of branching defects. These are interrogated by UV labeling, thus yielding the total number of defects for a given generation  $g$ , as accumulated during all synthetic steps. A theoretical treatment extracts the number of defects occurring at  $g$  from the total number of accumulated defects occurring for each member of a homologous series of DPs.<sup>35</sup> Interestingly, the onset of SIS is clearly seen when approaching the previously estimated  $g_{\max}$  range (Figure 2c). It is apparent upon comparison between two homologous series of DPs with  $g = 1–6$ , one with  $n \approx 50$  and the other with  $n \approx 1000$ . The shorter DPs are dendrimer-like because backbone end effects are dominant, while for the longer DPs end effects are negligible and the SIS reflects their cylindrical geometry. As expected from the estimated  $g_{\max}$ , the shorter DPs exhibit a constant near zero number of defects, while for the longer series, an upturn in the number of defects is evident for  $g > 4$ . This is manifested in the average number of junction-junction bonds per junction  $X_{\text{eff}}$ . At low  $g$ ,  $X_{\text{eff}} \lesssim 3$ , as expected for a near-perfect DP obtained from trifunctional dendronization units. The onset of SIS is manifested in a downturn of  $X_{\text{eff}}$  at  $g = 5$ , reaching  $X_{\text{eff}} = 2.89$  at  $g = 6$ , recalling that  $X_{\text{eff}}$  approaches  $X_{\text{eff}} = 2$  at  $g \gg g_{\max}$  when the SIS is strongest (Figure 2c). Gratifyingly, for the growth reaction to PG6 the total number of defects is still relatively small. We thus conclude that observing SIS near  $g_{\max}$  is in fact feasible, given our powerful chemistry that works reliably even under sterically rather unfavorable conditions.

What can be said about DPs of  $g > 6$  in the context of MO? While synthesis has meanwhile reached PG8,<sup>36</sup> obtaining credible data on shape, volume, and surface structure is a demanding undertaking and unfortunately somewhat lagging behind. Because we do not yet have a comprehensive set of experimental data on high  $g$  DPs we limit the discussion to results obtained by atomistic MD simulation.<sup>22,23</sup> Considering the large number of atoms involved and the simulation time, the results may reflect snapshots of nonequilibrated DPs rather than an equilibrium state corresponding to a free energy minimum. Nevertheless, it is likely that the simulations capture the gross structural features of the DPs. As expected, the average cross-section of PG6 and other high  $g$  DPs is circular. As was already discussed, the high- $g$  DPs have rather compact structures. This is also manifested in their radial density profiles displayed in Figure 3a for PG1–PG4 and PG6.<sup>22,23</sup> These profiles exhibit an extended inner plateau and then drop off sharply. The decay tails of the density profiles involve the outermost layers of the DPs with a thickness of roughly  $\approx 1$  nm independent of  $g$ . This outermost layer is associated with the “surface” of these objects and mediates their interactions.

Having discussed the shape and interfacial structure of DPs we turn to their shape persistence. To this end we compare the behavior of three systems upon adsorption to attractive solid substrates. It is established that adsorbed bottlebrush polymers, the counterparts of DPs with linear side chains, spread out almost completely with the side chains forming an adsorbed corona around the backbone (Figure 3c).<sup>37,38</sup> Thus, while bottlebrush polymers in a good solvent assume a locally cylindrical form similar to DPs, they are not shape persistent when “put to the test” by adsorption onto an attractive surface such as mica. When adsorbed these polymers flatten out and hence do not qualify as MOs. How about adsorbed DPs under similar conditions? A first impression is given by Figure 3d.<sup>15</sup> For all  $g$  depicted, the DP images have sharp edges as well as essentially constant,  $g$  specific widths and heights. Because of the importance of this issue for the entire discussion, the heights ( $h$ ) and widths ( $w$ ) of PG1–PG5 (PG6–PG8 will be reported soon) were quantitatively determined from TEM, SEM, and AFM images of single chains on solid mica and amorphous carbon substrates.<sup>15,28</sup> For PG5,  $h_{\text{TEM,mica}} = 7.3 \pm 0.2$  nm and  $w_{\text{SEM,C}} = 9.4 \pm 0.3$  nm were obtained (Figure 4a). Typical images used for this analysis are displayed in Figure 4b,c. There is in fact some departure from circular cross-section estimated to be in the range of  $\sim 25\%$ , assuming a density of  $\rho = 1.2$  g/cm<sup>3</sup>. To put this into perspective, we chose the tobacco mosaic virion (TMV) as a reference, because this self-assembled entity is reputed for its shape persistence.<sup>39</sup> Data on surface-induced flattening of TMV are scarce.<sup>40,41</sup> GISAXS measurements of TMV on strongly adsorbing SiO<sub>x</sub> led the authors to propose a flattening described as  $h/w \sim 0.57$ .<sup>40</sup> Though these values were obtained under different conditions and with different methods, it seems that PG5 does not flatten more than TMV, and this despite the fact that PG5 is not yet at  $g_{\text{max}}$ ! Finally, Figures 4d,e directly compare TMV and PG5 and highlight the ability of synthetic chemistry to create single, shape-retaining molecules having the size of mesoscopic biological functional entities without recourse to self-assembly. For this comparison notice that the TMV capsid proteins are the analogues of the dendrons and the RNA is the counterpart to the DP main chain. Note, however, that the TMV capsids are self-assembled onto the RNA scaffold, while the DP dendrons are covalently bound to the PMMA backbone.

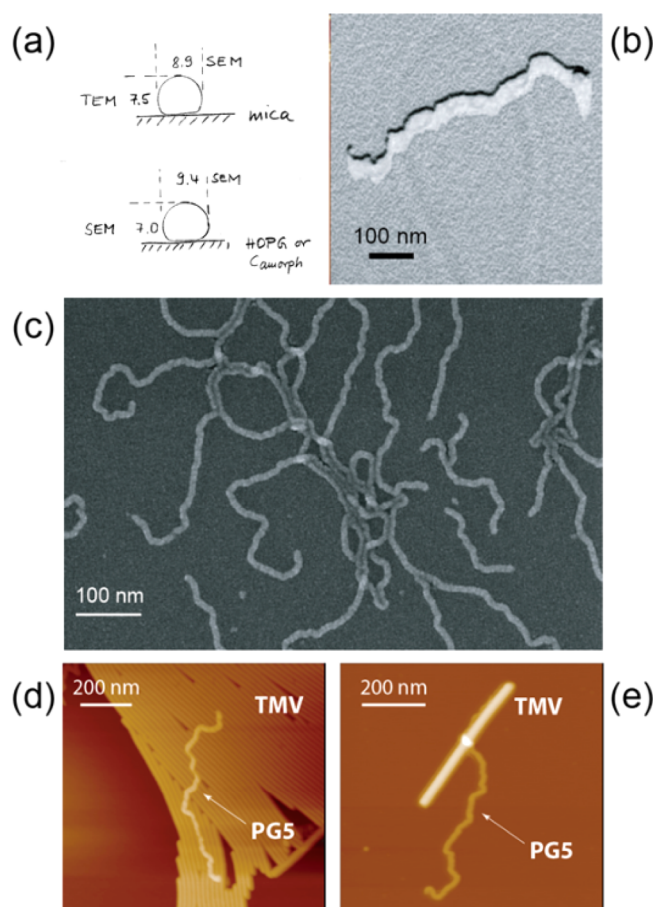


**Figure 4.** On the width and height of PG5. (a) Data on different substrates obtained by TEM and SEM of (b) unidirectionally and (c) rotary metal shadowed samples. (d) Comparison of apparent sizes, while deposited on an ordered array of TMVs and (e) when “embracing” a single virion.

Now that we have talked about branching defects, packing constraints, shape, and size, where do we stand? High  $g$  DPs of mesoscopic size basically maintain their shape even under external forces exercised by adsorbing surfaces. Size-wise, these single molecules are comparable to nanoparticles and by our definition they qualify as MOs. But how do DP MOs compare to polymeric colloids? What features justify differentiating between such colloidal particles and MOs? For simplicity, we restrict this discussion to a few examples beginning with simple PMMA or polystyrene (PS) beads, which can be obtained in sizes ranging from a few nm up to  $\approx 500$  nm. These beads contain a limited number of densely packed linear chains. Below the glass transition temperature ( $T_g$ ), the global motion of the chains is frozen and the beads exhibit hard sphere behavior. Surface treatment is required to prevent them from coagulation. Their spherical shape is a result of phase segregation during the preparation process utilizing suspension or emulsion polymerization. It does not reflect a molecular property of the polymer that forms the bead. The beads will dissolve in good solvent and can lose their shape upon heating to above  $T_g$ . In contrast, high  $g$  DPs retain their shape, even when exposed to good solvent or when heated to above  $T_g$ . This shape-persistence arises because these DPs are composed of one and only one molecule, thus, justifying their classification as MOs. In addition, these intriguing macromolecules have quantifiable structural perfection at least up to near  $g_{\text{max}}$ . When

compared to the polymeric beads, DPs have well-defined structure such that each dendron of the MO can be assigned to a specific volume element. Given an efficient synthetic strategy, DP MOs can be made virtually monodisperse in diameter without additional purification steps. Furthermore, the diameters of high  $g$  DPs should be fine-tuned in steps of roughly  $\approx 1$  nm from  $g$  to  $g + 1$  (Figure 5a). In contrast,

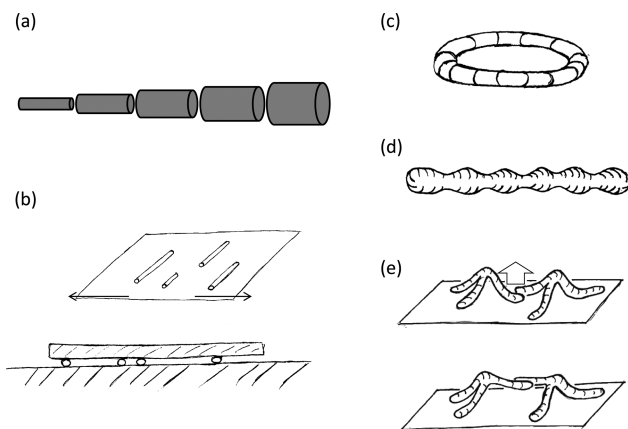


**Figure 5.** On the future of DP MOs. (a) A  $g$ -homologous set with increasing diameter. (b) Potential use for anisotropic lubrication. (c) A macrocycle MO and (d) a corrugated cylinder reminiscent of “colloidal molecules” obtained by self-assembly of patchy spherical particles. (e) Molecular construction exemplified by two three-armed DPs manipulated by AFM and then covalently “welded” photochemically.

colloidal particles produced with emulsion and miniemulsion techniques<sup>42</sup> are never fully monodispersed. In distinction to the beads mentioned earlier, the dissolution of DP MOs will not cause structural disintegration. Note, however, that cross-linking can render the multimolecular beads stable to dissolution. It is similarly instructive to compare DPs and polymeric micelles. In DPs above  $T_g$ , internal structure rearrangements constantly take place but do not affect the overall shape, while below  $T_g$  the structure is frozen. The effect of  $T$  on polymeric micelles brings up a new ingredient, namely, chain exchange, which occurs only above  $T_g$  of the insoluble component and has no counterpart in DPs. Another distinctive feature of DP concerns free ends. In contrast to block copolymer micelles, where each chain contributes two ends, the number of ends in DPs is comparable of the number of branched repeat units. This equips the DP MOs with an abundant number of active sites that can be used for conjugation as well as tuning solubility and melt behavior. The ends can dominate the solubility behavior when the DP MOs are exposed to a poor solvent for the branching units.

We next address the issue of whether DPs are the only MOs in the mesoscopic size range? While there are additional interesting candidate systems, their number is in fact rather limited and this article can be considered as an appeal for additional research. The first candidates to mention are spherical dendrimers near  $g_{\max}$ . Unfortunately there are only few cases where synthesis was pushed that far and with structure analysis. The 11th and 13th  $g$  dendrimers, reported respectively by Majoral/Caminade<sup>43</sup> and Simanek,<sup>44</sup> are noteworthy examples. Quantifying the defect statistics of these objects is yet to be completed. If one extends the scope beyond the synthetic realm, one may consider globular proteins

as MO candidates. However, in contrast to DPs, the shape of folded proteins is encoded into the monomer sequence, and they undergo denaturation upon heating, exposure to extreme pH or organic solvents, etc. To the extent one wishes to pursue peptide-based MOs using Merrifield-type synthesis, the current size limitation is at roughly hundred residues and thus below the mesoscopic range. Single or multiwalled carbon nanotubes may also be classified as MOs. Objects produced by 3D printing<sup>45</sup> or lithography techniques<sup>46</sup> are extrinsically shaped and thus excluded by our definition of MO.

In summary, high  $g$  DPs are unique macromolecules exhibiting shape persistence and dimensions reminiscent of colloidal or biological objects. Their size is tuned at the level of a single, covalent macromolecule. DP MOs of high  $g$  are characterized by an almost constant radial density profile with precisely defined connectivity, a combination permitting a unique tuning of their properties. For example, by changing  $g$  and the main chain length ( $n$ ), it is possible to vary their effective shape and interactions. Hence, DP structures span the range from conventional linear polymers at low- $g$  and large- $n$ , to spherical and cylindrical colloids obtained respectively at large- $g$  low- $n$  and large- $g$  large- $n$ . Moreover, DP MOs with their abundant active terminal groups can be used to simultaneously conjugate a variety of synthetic and biological entities as well as to control the binding of the conjugates.<sup>47–50</sup> DP afford a rich variety of topics for future research. One may for example explore on the lubrication effect of DP MOs when subject to shear. In particular, will their presence result in rolling or sliding, with possibilities for DP MOs acting as molecular cylindrical “roll bearings” (Figure 5b)? A step in this general direction investigated rolling and sliding of carbon nanotubes.<sup>51</sup> Another direction concerns DPs of different shapes. Thus, far the DP MOs we considered in this review are cylindrical. This however is not an obligatory restriction and low  $g$  DP tori were already reported (Figure 5c) by Grubbs and Grayson et al.<sup>52,53</sup> One may also consider corrugated DP MOs. A first step in this direction is the work of Chen et al.<sup>54</sup> on DPs with alternating copolymer backbones bearing dendrons of different size. While corrugated MOs (Figure 5d) are covalent structures, they are reminiscent of “colloidal molecules” obtained by self-assembly of patchy colloidal particles.<sup>55–59</sup> We suggest that the bulk viscosity of a melt of corrugated DP MOs depends on the mismatch between the lateral dimensions of the bumps and the dents, with higher viscosity expected when both features can go into register. Due to their unique molecular structure, DPs exhibit intriguing rheological aging behavior occurring without a corresponding chemical decomposition. Recent results suggest that this is related to a competition between inter- and intra-DP hydrogen bonding, but this is an open question that remains to be fully resolved.<sup>30,60–62</sup> The interfacial region of the DP MOs, where the radial density distribution decays from a plateau value to zero is likely to play an important role in this effect. These are but examples of further research opportunities involving DP rheology. There are additional directions to explore. The combination of shape-persistence and abundant functional groups gives rise to interesting possibilities when using photosensitive cross-linkable termini. In this situation it is possible to combine AFM manipulation with DP radiation induced “welding” to create higher order structures. This strategy was demonstrated on a surface where two individually adsorbed DPs were moved together and subsequently covalently joined.<sup>63,64</sup> With shape-persistent higher  $g$  DP one may envision the situation depicted in Figure

Se as an initial step in a similar construction strategy. Within it, the junction of a three-armed DP star will be lifted by an AFM tip thus forming an upward pointing “spike”. Subsequently, one arm of each two neighboring spikes will be lifted, brought into contact, and welded together photochemically to produce a tetrapod. This speculative procedure can be a step toward nanoconstruction with MOs. The illustrative examples listed above are by no means exhaustive. There are open questions concerning the bulk properties of DPs in the dry state. As a function of  $g$  and  $n$ , one anticipates various regimes such as liquid crystalline and glassy states. These aspects can be studied using X-ray diffraction and related techniques. The dynamics of DPs in solutions of different concentrations as well as the dry state remain to be explored using NMR and other relaxation spectroscopies. The configurations of individual DPs and the radial concentration profile of the dendron envelopes as well as their variation with  $g$  and  $n$  are yet to be systematically studied by scattering techniques such as SANS. Last, but not least, DP MOs provide an opportunity to revisit a fundamental question concerning the onset of macroscopic properties in single molecules. For example, is there a  $g$  such that a single MOs begins to exhibit a glass transition? From this viewpoint it would be of interest to combine calorimetric measurements with relaxation spectroscopies probing the dynamics of solutions of weakly interacting DP MOs noting possible complication because of solvent contributions to intra-MO dynamics.

## AUTHOR INFORMATION

### Notes

The authors declare no competing financial interest.

## ACKNOWLEDGMENTS

D.V. appreciates the hospitality and support of ETH during his sabbatical leave in fall 2013.

## REFERENCES

- Altintas, O.; Barner-Kowollik, C. *Macromol. Rapid Commun.* **2012**, *33*, 958.
- Sanchez-Sanchez, A.; Perez-Bena, I.; Pomposo, J. A. *Molecules* **2013**, *18*, 3339.
- McGraw-Hill Dictionary of Scientific and Technical Terms*, 6E; The McGraw-Hill Companies, Inc.; New York, 2003.
- Encyclopedia of Surface and Colloid Science*, 2nd ed.; Somasundran, P., Ed.; CRC Press Taylor & Francis: Boca Raton, FL, 2006.
- Biochemistry*, 3rd ed.; Voet, D., Voet, J. G., Eds.; Wiley & Sons Inc.: Hoboken, NJ, 2004.
- Freudenberger, R.; Claussen, W.; Schlüter, A. D.; Wallmeier, H. *Polymer* **1994**, *35*, 4496.
- Schlüter, A. D.; Rabe, J. *Angew. Chem., Int. Ed.* **2000**, *39*, 864.
- Frauenrath, H. *Prog. Polym. Sci.* **2005**, *30*, 325.
- Schlüter, A. D. *Top. Curr. Chem.* **2005**, *245*, 151.
- Birshstein, T. M.; Borisov, O. V.; Zhulina, E. B.; Khokhlov, A. R.; Yurasova, T. A. *Polym. Sci. USSR* **1987**, *29*, 1293.
- Potemkin, I. I.; Khokhlov, A. R.; Reineker, P. *Eur. Phys. J. E* **2001**, *4*, 93.
- Zhang, M. F.; Müller, A. H. E. *J. Polym. Sci., Polym. Chem.* **2005**, *43*, 2005.
- Sheiko, S. S.; Sumerlin, B. S.; Matyjaszewski, K. *Prog. Polym. Sci.* **2008**, *33*, 759.
- Newkome, G. R.; Moorefield, C. N.; Vögtle, F. *Dendrimers and Dendrons: Concepts, Syntheses, Applications*; Wiley-VCH: Weinheim, 2001.
- Zhang, B.; Wepf, R.; Fischer, K.; Schmidt, M.; Besse, S.; Lindner, P.; King, B. T.; Sigel, R.; Schurtenberger, P.; Talmon, Y.; Ding, Y.; Kröger, M.; Halperin, A.; Schlüter, A. D. *Angew. Chem., Int. Ed.* **2011**, *50*, 737.
- Buhleier, E.; Wehner, W.; Vögtle, F. *Synthesis* **1978**, 155–158.
- Tomalia, D. A.; Baker, H.; Kallós, G.; Martin, S.; Smith, P. *Polym. J.* **1985**, *17*, 117–132.
- Erikson, B. W.; Merrifield, R. B. In *The Proteins*; Neurath, H., Hill, R. L., Eds.; Academic Press: New York, 2012; Vol. 2, p 259.
- Grosberg, A. Y.; Khokhlov, A. R. *Statistical Physics of Macromolecules*; American Institute of Physics: New York, 1994.
- Guo, Y.; van Beek, J. D.; Zhang, B.; Colussi, M.; Walde, P.; Zhang, A.; Kröger, M.; Halperin, A.; Schlüter, A. D. *J. Am. Chem. Soc.* **2009**, *131*, 11841.
- Zhulina, E. B.; Birshstein, T. M. *Polym. Sci. USSR (Engl. Transl.)* **1985**, *27*, 570.
- Bertran, O.; Zhang, B.; Schlüter, A. D.; Halperin, A.; Kröger, M.; Aleman, C. *RSC Adv.* **2013**, *3*, 126.
- Bertran, O.; Zhang, B.; Schlüter, A. D.; Kröger, M.; Aleman, C. *J. Phys. Chem. B* **2013**, *117*, 6007.
- DeGennes, P. G.; Hervet, H. *J. Phys., Lett.* **1983**, *44*, L351.
- Tomalia, D. A. *New J. Chem.* **2012**, *36*, 264.
- Tomalia, A. D. *Adv. Polym. Sci.* **2013**, *261*, 321–390.
- Kröger, M.; Schlüter, A. D.; Halperin, A. *Macromolecules* **2013**, *46*, 7550–7564.
- Zhang, B.; Wepf, R.; Kröger, M.; Halperin, A.; Schlüter, A. D. *Macromolecules* **2011**, *44*, 6785.
- Kröger, M.; Peleg, O.; Halperin, A. *Macromolecules* **2010**, *43*, 6213–6224.
- Kröger, M.; Zhang, B.; Rosenauer, C.; Schlüter, A. D.; Wegner, G. *Colloid Polym. Sci.* **2013**, *12*, 2879.
- Rosen, B. M.; Wilson, C. J.; Wilson, D. A.; Peterca, M.; Imam, M. R.; Percec, V. *Chem. Rev.* **2009**, *109*, 6275.
- Tomalia, D. A.; Naylor, A. M.; Goddard, W. A., III *Angew. Chem., Int. Ed.* **1990**, *29*, 138.
- Lothian-Tomalia, M. K.; Hedstrand, D. M.; Tomalia, D. A.; Padias, A. B.; Hall, H. K., Jr *Tetrahedron* **1997**, *53*, 15495.
- Tomalia, D. A.; Christiansen, J. B.; Boas, U. *Dendrimers, Dendrons, and Dendritic Polymers: Discovery, Applications, the Future*; Cambridge Univ. Press: Cambridge, 2012.
- Zhang, B.; Yu, H.; Schlüter, A. D.; Halperin, A.; Kröger, M. *Nat. Commun.* **2013**, *4*, 1993.
- Yu, H.; Schlüter, A. D.; Zhang, B. *Macromolecules* **2014**, *47*, 4127.
- Sheiko, S. S.; Möller, M. *Chem. Rev.* **2001**, *101*, 4099.
- Panyukov, S.; Zhulina, E. B.; Sheiko, S. S.; Randall, G. C.; Brock, J.; Rubinstein, M. *J. Phys. Chem. B* **2009**, *113*, 3750.
- Ref 5, p 1377.
- Lee, B.; Lo, C.-T.; Thiyagarajan, P.; Winans, R. E.; Li, X.; Niu, Z.; Wang, Q. *Langmuir* **2007**, *23*, 11157.
- Knez, M.; Sumser, M. P.; Bittner, A. M.; Wege, C.; Jeske, H.; Hoffmann, D. M. P.; Kuhnke, K.; Kern, K. *Langmuir* **2004**, *20*, 441.
- Landfester, K.; Crespy, D. In *Synthesis of Polymers, New Structures and Methods*; Schlüter, A. D., Hawker, C. J., Sakamoto, J., Eds.; Wiley-VCH: Weinheim, 2012; p 449.
- Lartigue, M.-L.; Donnadieu, B.; Galliot, C.; Caminade, A.-M.; Majoral, J.-P.; Fayet, J.-P. *Macromolecules* **1997**, *30*, 7335.
- Lim, J.; Kostianen, M.; Maly, J.; da Costa, V. C. P.; Annunziata, O.; Pavan, G. M.; Simanek, E. E. *J. Am. Chem. Soc.* **2013**, *135*, 4660.
- Sun, K.; Wei, T.-S.; Ahn, B. Y.; Seo, J. Y.; Dillon, S. J.; Lewis, J. A. *Adv. Mater.* **2013**, *25*, 4539–4543.
- Bertsch, A.; Lorenz, H.; Renaud, P. *Sens. Actuators* **1999**, *73*, 14.
- Fornera, S.; Balmer, T. E.; Zhang, B.; Schlüter, A. D.; Walde, P. *Macromol. Biosci.* **2011**, *11*, 1052.
- Fornera, S.; Bauer, T.; Schlüter, A. D.; Walde, P. *J. Mater. Chem.* **2012**, *22*, 502.
- Fornera, S.; Kuhn, P.; Lombardi, D.; Schlüter, A. D.; Dittrich, P. S.; Walde, P. *ChemPlusChem* **2012**, *77*, 98.
- Grotzky, A.; Nauser, T.; Erdogan, H.; Schlüter, A. D.; Walde, P. *J. Am. Chem. Soc.* **2012**, *134*, 11392.

- (51) Falvo, M. R.; Taylor, R. M., II; Helsler, A.; Chi, V.; Brooks, F. P., Jr; Washburn, S.; Superfine, R. *Nature* **1999**, *397*, 236.
- (52) Boydston, A. J.; Holcombe, T. W.; Unruh, D. A.; Fréchet, J. M. J.; Grubbs, R. H. *J. Am. Chem. Soc.* **2009**, *131*, 5388.
- (53) Laurant, B. A.; Grayson, S. M. *J. Am. Chem. Soc.* **2011**, *133*, 13421.
- (54) Chen, Y. M.; Xiong, X. Q. *Chem. Commun.* **2010**, *46*, 5049.
- (55) Nelson, D. R. *Nano Lett.* **2002**, *2*, 1125–1129.
- (56) Monoharan, V. N.; Elsesser, M. T.; Pine, D. J. *Science* **2003**, *301*, 483–487.
- (57) Yi, G. R.; Pine, D. J.; Sacanna, S. *J. Phys.: Condens. Matter* **2013**, *25*, 193101.
- (58) Bianchi, E.; Largo, J.; Tartaglia, P.; Zaccarelli, E.; Sciortino, F. *Phys. Rev. Lett.* **2006**, *97*, 168301.
- (59) Bianchi, E.; Blaak, R.; Likos, C. N. *Phys. Chem. Chem. Phys.* **2011**, *13*, 6397.
- (60) Zhang, A.; Okrasa, L.; Pakula, T.; Schlüter, A. D. *J. Am. Chem. Soc.* **2004**, *126*, 6658.
- (61) Pasquino, R.; Zhang, B.; Sigel, R.; Yu, H.; Ottiger, M.; Bertran, O.; Aleman, C.; Schlüter, A. D.; Vlassopoulos, D. *Macromolecules* **2012**, *45*, 8823.
- (62) Cordova-Mateo, E.; Bertran, O.; Zhang, B.; Vlassopoulos, D.; Pasquino, R.; Schlüter, A. D.; Kröger, M.; Aleman, C. *Soft Matter* **2014**, *10*, 1032.
- (63) Barner, J.; Mallwitz, F.; Shu, L.; Schlüter, A. D.; Rabe, J. P. *Angew. Chem., Int. Ed.* **2003**, *42*, 1932.
- (64) Al-Hellani, R.; Barner, J.; Rabe, J. P.; Schlüter, A. D. *Chem.—Eur. J.* **2006**, *12*, 6542.